

Tuning Models of Pilot Tracking Behavior for a Specific Simulator Motion Cueing Setting

D.M. Pool,^{*} H.J. Damveld,[†] M.M. van Paassen,[‡] and M. Mulder[§]

Delft University of Technology, Delft, The Netherlands

This paper describes the preliminary results of an effort to compile data from a large number of studies that investigated the effects of variations in motion filter settings on pilot behavior. The main objective of this study is to formulate a set of mathematical rules that will allow for the tuning of behavioral pilot models to a certain motion cueing setting. To achieve this, data for different dependent measures such as tracking performance, pilot-vehicle system crossover frequencies, and pilot model parameters, taken from ten different experiments that considered pilot tracking behavior under varying rotational or translational motion cueing settings, has been combined. By checking the correlation of the variation in any of these dependent measures and parameters that quantify the applied variation in motion cueing, a number of consistent relations has been identified. The most consistent and clear effects that are found from this analysis are variations in some important dependent measures with the motion filter gain at 1 rad/s. Over the full range of motion filter gains at 1 rad/s from 0 to 1, a reduction in pilot visual gain of around 20% is observed with reducing motion filter gain, in combination with a 30% increase in the amount of visual lead equalization adopted by pilots.

Nomenclature

E	Fourier transform of e	K	Motion filter gain
e	Tracking error signal	K_m	Pilot motion gain
f_d	Disturbance forcing function	K_S	Motion filter gain at 1 rad/s
f_t	Target forcing function	K_s	Pilot control scaling gain
H_c	Controlled dynamics	K_v	Pilot visual gain
H_{e,f_d}	Closed-loop disturbance-to-error dynamics	n	Remnant signal
H_{e,f_t}	Closed-loop target-to-error dynamics	R	Correlation coefficient
H_m	Motion perception/equalization dynamics	s	Laplace operator
H_{mf}	Motion filter dynamics	T_I	Pilot visual lag time constant
H_{nm}	Neuromuscular system dynamics	T_L	Pilot visual lead time constant
$H_{ol,d}$	Disturbance open-loop dynamics	U_c	Fourier transform of u_c
$H_{ol,t}$	Target open-loop dynamics	u	Pilot control signal
H_{pv}	Pilot visual response	u_c	Scaled pilot control signal
H_{pm}	Pilot motion response	X	Fourier transform of x
H_{s_v}	Simulator visual cueing dynamics	x	Controlled element state
H_{s_m}	Simulator motion cueing dynamics	Y	Generic motion fidelity metric
$H_{\dot{y},x}$	Controlled motion dynamics	\dot{y}	Motion feedback signal
H_c	Controlled element dynamics	Z	Generic dependent measure
j	Imaginary unit		

^{*}PhD Student, Control and Simulation Division, Faculty of Aerospace Engineering, P.O. Box 5058, 2600GB Delft, The Netherlands; d.m.pool@tudelft.nl. Member AIAA.

[†]Postdoctoral Research Fellow, Control and Simulation Division, Faculty of Aerospace Engineering, P.O. Box 5058, 2600GB Delft, The Netherlands; h.j.damveld@tudelft.nl. Member AIAA.

[‡]Associate Professor, Control and Simulation Division, Faculty of Aerospace Engineering, P.O. Box 5058, 2600GB Delft, The Netherlands; m.m.vanpaassen@tudelft.nl. Member AIAA.

[§]Professor, Control and Simulation Division, Faculty of Aerospace Engineering, P.O. Box 5058, 2600GB Delft, The Netherlands; m.mulder@tudelft.nl. Member AIAA.

Symbols

$\alpha_{Y_{ref}}$	Linear regression offset
β	Linear regression coefficient
δ_c	Controlled element input
ζ_n	Motion filter damping ratio
ζ_{nm}	Neuromuscular damping ratio
σ_e^2	Tracking error variance
σ_u^2	Pilot control signal variance
τ_m	Pilot motion time delay, s
τ_v	Pilot visual time delay, s
$\varphi_{m,d}$	Disturbance phase margin, deg
$\varphi_{m,t}$	Target phase margin, deg

ϕ_S	Motion filter phase at 1 rad/s, deg
ω	Frequency, rad/s
ω_b	Motion filter second break frequency, rad/s
$\omega_{c,d}$	Disturbance crossover frequency, rad/s
$\omega_{c,t}$	Target crossover frequency, rad/s
ω_n	Motion filter break frequency, rad/s
ω_{nm}	Neuromuscular frequency, rad/s

Subscripts

—	Normalized
1	For $K_S = 1$
<i>ref</i>	Predictor reference setting

I. Introduction

Much of our current knowledge on human manual control behavior has come from the considerable database of behavioral measurements that have been collected for single-loop compensatory tracking tasks.¹ Using this extensive database, it has been shown that single-loop pilot tracking behavior during compensatory tracking tasks can be modeled at high accuracy using quasi-linear pilot models.^{1,2} The fitting of such quasi-linear pilot models to measurements of pilot tracking behavior has allowed for a quantitative evaluation of changes in pilot dynamics due to a number of different factors, thereby increasing our understanding of human operation during manual control. Furthermore, rules have been developed that allow for intuitive tuning of such single-loop models of pilot tracking behavior to the defining features of the considered control task, such as the dynamics of the controlled element and the characteristics of the applied forcing function signals.^{1,2} This set of rules thereby allows for prediction of pilot control behavior during tracking for certain combinations of controlled elements and forcing function signals without having to resort to experimental evaluation of pilot control behavior and has shown its merit in various areas of human-machine interaction research.

The presence of physical motion feedback of the controlled element state has been shown to yield pilot control behavior during compensatory control tasks that is markedly different from that observed for single-loop tasks where motion feedback is not available.^{3,4} A research question that is currently of interest to the flight simulation community is how, and to what extent, pilot tracking behavior is affected by the usage of simulator motion cueing strategies as commonly adopted in full-motion flight simulation.^{5,6} To answer this question, and to allow for the prediction of changes in pilot behavior due to a selected simulator motion cueing strategy, a set of rough tuning rules for incorporating the approximate effects of cueing settings on pilot behavior into pilot models – preferably validated through extensive experimental measurements – would be a valuable tool. Unfortunately, largely due to the complexity of human perceptual processes and manual control behavior in multimodal environments, such a standardized set of rules for pilot model tuning that includes the effects of the supplied physical motion cues does not exist yet.

A large research project at Delft University of Technology attempts to contribute to solving this problem by tracing observed changes in measured pilot tracking behavior during tracking tasks with physical motion feedback back to the selected flight simulator motion cueing settings.⁷ The final objective of this study is to use these measurements of pilot behavior, and a comparison with measurements of true in-flight tracking behavior, to define a behavioral flight simulator motion fidelity criterion. Given a certain control task or maneuver, this criterion is meant to allow for selecting a flight simulator motion cueing setting that will yield pilot behavior that is as close to that observed in real flight as possible. Despite not being representative for all aspects of aircraft control, compensatory tracking tasks where physical motion feedback is available in addition to visual error information are used in this study to evaluate the underlying multimodal motion perception and integration processes that are important during manual aircraft control. Similar to the single-loop case studied by McRuer et al.,¹ these multimodal tracking tasks have been shown to allow for the modeling, and thereby the explicit quantification, of changes in pilot control strategy by using quasi-linear multimodal pilot models.^{4,8}

This paper provides the first result of our effort in compiling data from a number of experiments from which measurements of multimodal pilot behavior under varying motion cueing conditions are available. Data have been collected from a number of investigations performed at Delft University of Technology^{7,9-12} and from a number of studies found in literature.^{4,8,13-15} This paper will provide a short overview of the scope and setup of all these different experiments. The main objective of this paper, however, is to use the total set of collected data to identify consistent trends in typical dependent measures of pilot control strategy and the parameters that define the applied motion cueing

setting. The main dependent measures by which the effect of simulator motion cueing on pilot tracking behavior will be evaluated in this paper are:

1. tracking performance and control activity
2. pilot-vehicle system crossover frequencies and phase margins
3. identified multimodal pilot model parameters

A relation is sought between these different dependent measures of pilot tracking behavior and typical metrics that quantify the level of simulator motion attenuation by the motion filter. Examples of metrics that are considered are the motion filter parameters (gain, break frequency) and motion filter gain and phase distortion at a certain frequency, for example, the 1 rad/s evaluation frequency proposed by Sinacori.¹⁶ A rudimentary set of pilot model tuning rules will be obtained by fitting a linear regression through combinations of dependent measures and motion fidelity metrics for which a clear correlation is present.

II. Background

II.A. Simulator Motion Fidelity

Due to severe limitations on the motion capabilities of flight simulators, motion washout algorithms are required for attenuating and limiting the simulated aircraft motion. A large diversity in washout algorithms has been developed over the years.¹⁷⁻¹⁹ One of the biggest challenges facing the flight simulation community, however, has been finding an appropriate criterion for the evaluation of simulator motion cueing fidelity and defining the minimum requirements for simulator motion cueing for pilot training and other flight simulator applications.

One of the first efforts to define a structured and practical methodology for the assessment of simulator motion fidelity was the work of Sinacori,¹⁶ who proposed a motion fidelity criterion based on the combination of motion filter gain and phase distortion introduced by motion filters at a frequency of 1 rad/s. This frequency, though still the topic of much debate, was selected as much of the activity during manual aircraft control was thought to be centered around this frequency range. The criterion proposed by Sinacori was later modified and validated by Schroeder²⁰ using subjective motion fidelity assessments for various helicopter tasks.

Hess et al.²¹ defined a more analytical methodology for evaluating simulator motion fidelity from the effect of a motion filter on the dynamics of the combined simulator, aircraft, and pilot system in a flight simulator. For a helicopter lateral translational maneuver, Hess et al. showed that their chosen criterion was indeed sensitive to variations in motion cueing fidelity. Hess and Marchesi²² later showed this analytical method to also be applicable to other types of aircraft and maneuvers.

The most recent effort into the formulation of a standard for the assessment of flight simulator motion fidelity is the work of Advani and Hosman.²³ Their proposed motion fidelity criterion, which is currently being included in the ICAO 9625 manual for the qualification of flight simulator devices, considers the dynamics of the simulator motion hardware in addition to those of the motion cueing algorithm, and evaluates the total motion cueing dynamics over a frequency range that is thought to be important for manual aircraft control.

The work described in this paper is part of a research effort that attempts to develop a framework for assessing simulator motion fidelity from measurements of pilot control behavior.⁷ By measuring changes in pilot control behavior that result from applied changes in simulator motion cueing, as opposed to relying on subjective motion fidelity rating procedures, it is hoped that some experimental validation of the criteria proposed for evaluating simulator motion fidelity can be provided.

II.B. Pilot Tracking Behavior

Fig. 1 shows a generalized and extensive schematic representation of a closed-loop aircraft manual tracking task performed in a flight simulator environment, which is valid for the tracking tasks performed in all of the studies into the effects of motion filter dynamics on pilot behavior considered in this paper. The target and disturbance forcing function signals that induce pilot tracking behavior and thereby define the type of tracking task under consideration (target following, disturbance rejection, or the combination of both) are depicted in Fig. 1 with the symbols f_t and f_d , respectively. As can be verified from Fig. 1, a distinction is made between simulator, pilot, and controlled element dynamics. Simulator dynamics include the characteristics of the simulator visual and simulator motion cueing systems

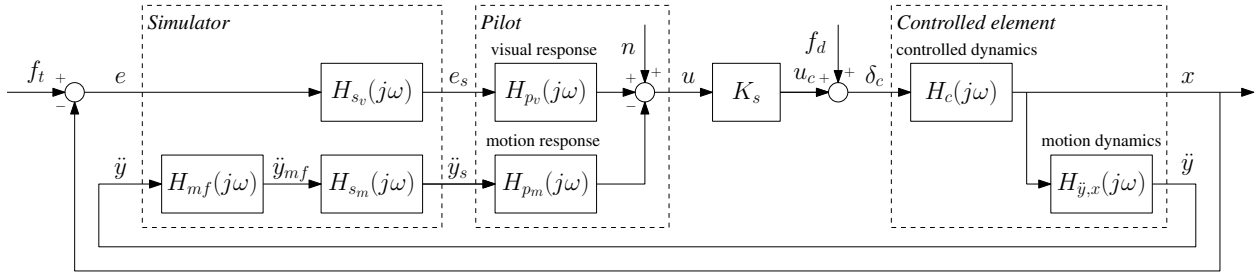


Figure 1. Schematic representation of a compensatory tracking task with motion feedback.

($H_{sv}(j\omega)$ and $H_{sm}(j\omega)$, respectively), in addition to the dynamics of the applied motion filter which are indicated by the $H_{mf}(j\omega)$ block.

As can be verified from Fig. 1, this study considers control tasks for which pilot control behavior can be represented as the sum of two parallel responses to visual and motion information.⁸ The pilot visual response $H_{pv}(j\omega)$ captures pilots' control dynamics in response to presented tracking errors e_s , while the pilot motion response $H_{pm}(j\omega)$ models pilots' responses to cued motion information \ddot{y}_s . The remnant signal n , which accounts for all nonlinear contributions to the pilot control input u ,² completes this quasi-linear model of pilot tracking behavior.

The controlled element dynamics are defined to consist of two separate parts: the controlled dynamics and the motion dynamics. The former, $H_c(j\omega)$, are the dynamics that drive the vehicle state that is controlled by the pilot, x . The motion dynamics $H_{\ddot{y},x}(j\omega)$ define the transformation from the controlled state x to the variable that enters the pilot's motion response channel $H_{pm}(j\omega)$. When $H_{pm}(j\omega)$ captures pilots' responses to angular or translational cues perceived through the vestibular system (through the semicircular canals or otoliths, respectively)²⁴ – as is the case for most control tasks considered in this paper – motion cueing provides pilots with feedback of the acceleration of the controlled element state, so $H_{\ddot{y},x}(j\omega) = (j\omega)^2$. However, more extensive transformations between controlled state and motion feedback quantities exist in some studies, for instance for the aircraft pitch control tasks with variation in the coupled heave motion cueing considered in Refs. 11 and 25. Note that a further scaling of pilot control inputs, resulting from a control scaling gain K_s , is present in some of the considered studies.

II.C. Motion Fidelity and Tracking Behavior

As can be verified from Fig. 1, the closed-loop pilot-vehicle system dynamics in a closed-loop control task will be affected by the presence of a motion filter. For instance, the following relations can be derived from Fig. 1 for the disturbance and target open-loop responses, whose crossover frequencies and phase margins can be used for assessing closed-loop pilot-vehicle system performance and stability for disturbance rejection and target-following, respectively.⁴

$$H_{ol,d}(j\omega) = -\frac{U_c(j\omega)}{\delta_c(j\omega)} = [H_{sv}(j\omega)H_{pv}(j\omega) + H_{\ddot{y},x}(j\omega)H_{mf}(j\omega)H_{sm}(j\omega)H_{pm}(j\omega)] K_s H_c(j\omega) \quad (1)$$

$$H_{ol,t}(j\omega) = \frac{X(j\omega)}{E(j\omega)} = \frac{H_{sv}(j\omega)H_{pv}(j\omega)K_s H_c(j\omega)}{1 + H_{\ddot{y},x}(j\omega)H_{mf}(j\omega)H_{sm}(j\omega)H_{pm}(j\omega)K_s H_c(j\omega)} \quad (2)$$

Similarly, the corresponding closed-loop forcing function to error responses, which are indicative of the success of the closed-loop system depicted in Fig. 1 in attenuating f_d and following f_t , are given by:

$$H_{e,f_d}(j\omega) = \frac{E(j\omega)}{F_d(j\omega)} = \frac{-H_c(j\omega)}{1 + [H_{sv}(j\omega)H_{pv}(j\omega) + H_{\ddot{y},x}(j\omega)H_{mf}(j\omega)H_{sm}(j\omega)H_{pm}(j\omega)] K_s H_c(j\omega)} \quad (3)$$

$$H_{e,f_t}(j\omega) = \frac{E(j\omega)}{F_t(j\omega)} = \frac{1 + H_{\ddot{y},x}(j\omega)H_{mf}(j\omega)H_{sm}(j\omega)H_{pm}(j\omega)K_s H_c(j\omega)}{1 + [H_{sv}(j\omega)H_{pv}(j\omega) + H_{\ddot{y},x}(j\omega)H_{mf}(j\omega)H_{sm}(j\omega)H_{pm}(j\omega)] K_s H_c(j\omega)} \quad (4)$$

First of all, Equations (1) to (4) indicate that the effect of the motion filter dynamics $H_{mf}(j\omega)$ on these open-loop and closed-loop relations depends on the dynamics of all other elements shown in Fig. 1. In addition, compared to

the case where no motion filter is present ($H_{mf}(j\omega) = 1$), pilots may adapt their control dynamics in response to a motion filter with certain dynamics being introduced to (partially) compensate for the effect the motion filter dynamics have on the closed-loop system. The most elementary example that can be given is the case where motion cues are attenuated by a pure gain, $H_{mf}(j\omega) = K$. As long as the gain does not cause the motion cues to become smaller than human motion perception thresholds,¹⁰ pilots could simply respond to the lower magnitude motion information (\dot{y}_s) with a higher gain. If they succeed in increasing the gain of $H_{pm}(j\omega)$ with around $1/K$, this means the governing open-loop and closed-loop dynamics remain approximately the same, as can be verified from Eqs. (1) to (4).

Much like the work of Hess et al.,²¹ this project is concerned with the effects of the presence of a motion filter on the dynamics of the closed-loop pilot-vehicle system as depicted in Fig. 1. However, unlike previous work on this topic, the focus is on how these changes in the closed-loop tracking task dynamics induce changes in pilot control behavior, to partially alleviate the effects of the motion filter dynamics on the closed-loop characteristics, and to obtain quantitative measurements of these changes in pilot behavior from human-in-the-loop evaluations.⁷

III. Method

III.A. Selection Criteria: Dependent Measures

A large number of studies have been dedicated to the evaluation of the effects of simulator motion cueing on pilot performance, motion perception, and control behavior. An excellent recent overview of a large number of these studies is given by Schroeder and Grant.⁵ For the current paper, only a specific subset of the large body of literature on the effects of motion filters is of interest due to the focus on measured changes in pilot behavior. The main requirement for a study to be included in this overview is that it should provide some behavioral measurement over a number of different motion cueing conditions, most preferably through models of pilots' dynamical responses ($H_{pv}(j\omega)$ and $H_{pm}(j\omega)$), as defined in Fig. 1). These dynamical pilot responses are typically modeled with linear models that can be deduced from or are equivalent to the equations given by:

$$H_{pv}(j\omega) = K_v \frac{(1 + T_L j\omega)^2}{1 + T_I j\omega} e^{-j\omega\tau_v} H_{nm}(j\omega) \quad (5)$$

$$H_{pm}(j\omega) = K_m H_m(j\omega) e^{-j\omega\tau_m} H_{nm}(j\omega) \quad (6)$$

$$H_{nm}(j\omega) = \frac{1}{\left(\frac{j\omega}{\omega_{nm}}\right)^2 + \frac{2\zeta_{nm}}{\omega_{nm}} j\omega + 1} \quad (7)$$

Eq. (5) defines the most elaborate form of the modeled pilot response to visual cues considered in this study, consisting of a pure gain, a lead-lag equalization element, a pure delay term, and the low-pass neuromuscular actuation dynamics model given by Eq. (7). As detailed in Ref. 26 the full lead-lag equalization element shown Eq. (5) is required for capturing pilot dynamics during control of certain conventional aircraft pitch dynamics, but may, for instance, be reduced to a pure first-order lead or a pure gain for controlled elements that have approximately double or single integrator dynamics in the crossover region, respectively.¹

For modeling of pilots' responses to motion information, typically models of the form of Eq. (6) are adopted. Similar to the model for the pilot visual response, these models also include pure gain and pure delay terms and the same neuromuscular actuation model. In addition, Eq. (6) includes the further unspecified $H_m(j\omega)$ terms, which represents further possible contributions to the pilot motion dynamics $H_{pm}(j\omega)$ such as (vestibular) sensory dynamics and possible equalization dynamics, similar to the lead-lag element in Eq. (5). In this study, we limit ourselves to the measurements of the pilot motion gain K_m and delay τ_m , that is, changes in these further dynamics of pilots' motion responses are not considered.

Table 1 lists the full set of dependent measures selected for the overview of motion filter effects provided by this paper. In addition to the parameters of the considered behavioral models of pilot behavior listed in the final column of Table 1, two additional groups of dependent measures are considered: performance measures and pilot-vehicle system crossover characteristics. In many studies into the effects of motion cueing on pilot behavior, performance measures such as the variance of the recorded tracking error and control signals are considered as dependent measures, as these metrics are often found to signal underlying changes in pilot behavior. Similarly, pilot-vehicle system crossover parameters reveal how possible changes in pilot behavior affect the dominant characteristics of the combined open-loop

Table 1. Considered dependent measures.

Performance Measures		Crossover Characteristics		Pilot Behavioral Parameters	
Symbol	Definition	Symbol	Definition	Symbol	Definition
σ_e^2	Tracking error variance	$\omega_{c,d}$	Disturbance crossover frequency	K_v	Pilot visual (error) gain
σ_u^2	Control input variance	$\omega_{c,t}$	Target crossover frequency	T_L	Pilot visual lead time constant
		$\varphi_{m,d}$	Disturbance phase margin	T_I	Pilot visual lag time constant
		$\varphi_{m,t}$	Target phase margin	$K_v T_L$	Pilot visual lead gain
				K_m	Pilot motion gain
				τ_m	Pilot visual delay
				τ_m	Pilot motion delay
				ω_{nm}	Neuromuscular system natural frequency
				ζ_{nm}	Neuromuscular system damping ratio

pilot-vehicle system in the important frequency range around gain crossover.¹ Note that due to the different open-loop response definition for target-following and disturbance-rejection tasks,⁴ see Equations (1) and (2), crossover frequencies and phase margins for both target-following and disturbance-rejection loops are separated. Furthermore, this implies that for studies that consider pure target-following or disturbance-rejection tasks only one set of crossover frequencies and phase margins is available.

III.B. Predictors: Motion Fidelity Measures

For attenuating the simulated aircraft motion and for washing out flight simulator motion typically a combination of pure gain attenuation and high-pass filtering is adopted in flight simulation.¹⁷ Due to the fact that the required amount of attenuating and filtering is highly dependent on the vehicle, maneuver, simulator axis, and perhaps even the pilot who is executing the maneuver, there is quite some variation in the dynamics of the adopted washout filter dynamics ($H_{mf}(j\omega)$ in Fig. 1). For the studies considered in this paper, washout dynamics vary from 0th order (pure gain) to 3rd order high-pass filters:

$$0^{\text{th}} \text{ order: } H_{mf}(s) = K \quad (8)$$

$$1^{\text{st}} \text{ order: } H_{mf}(s) = K \frac{s}{s + \omega_n} \quad (9)$$

$$2^{\text{nd}} \text{ order: } H_{mf}(s) = K \frac{s^2}{s^2 + 2\zeta_n \omega_n s + \omega_n^2} \quad (10)$$

$$3^{\text{rd}} \text{ order: } H_{mf}(s) = K \frac{s^2}{s^2 + 2\zeta_n \omega_n s + \omega_n^2} \frac{s}{s + \omega_b} \quad (11)$$

The washout filter order has a dominant effect on the level of fidelity of the supplied simulator motion cues. For constant parameter settings, motion fidelity decreases with increasing filter order, as increasingly more low-frequency motion is attenuated and phase distortion increases rapidly for higher order filters. The level of motion fidelity is of course also affected by the parameters of the different washout filters listed in Eq. (8) to (11) define the level of supplied motion fidelity. Generally higher filter gains K and lower (dominant) break frequencies ω_n correspond to higher fidelity motion cueing.¹⁶

The objective of this study is to relate measured changes in any of the dependent measures listed in Table 1 to some important measure of simulator motion fidelity. If a clear correlation exists between some combination of dependent measure and fidelity measure, this means this fidelity measure can be used as a predictor of the observed change in the dependent measure. A natural first choice for measures of motion fidelity are of course the washout filter parameters: the filter gain K , the filter break frequency ω_n , the filter damping ratio ζ_n , and the additional first-order filter break frequency ω_b . The dominant parameters with the largest effect on the washout filter dynamics are the filter gain K and the filter break frequency ω_n . Hence, these two parameters were selected as a first set of possible predictor variables.

Filter parameters, however, do not account for the effect of filter order. This makes comparison of the level of motion fidelity by evaluating these parameters between studies with different order washout filters difficult. This was

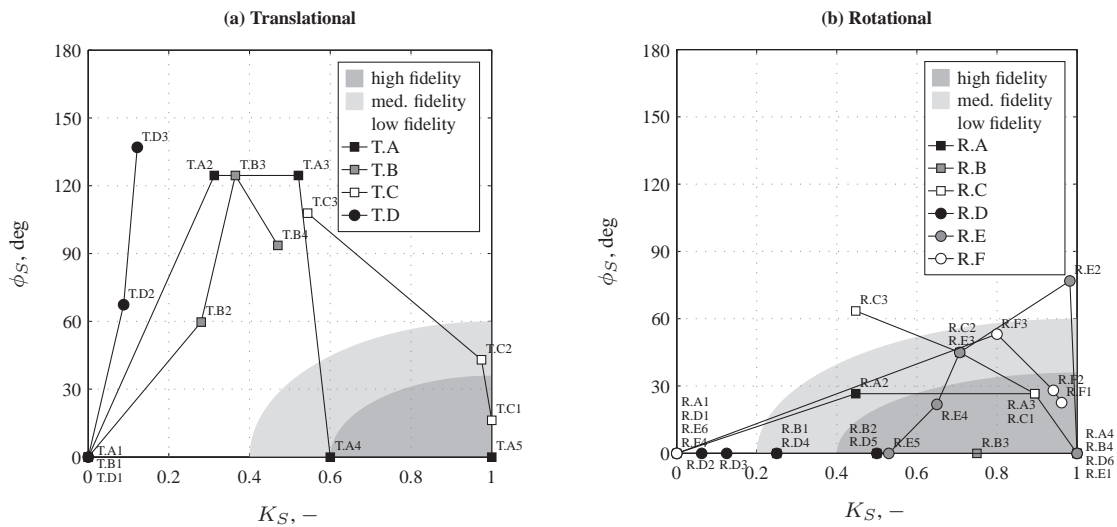


Figure 2. Compiled translational and rotational motion filter settings from literature.

also recognized by Sinacori, who therefore proposed the usage of the gain and phase distortion at a frequency of 1 rad/s induced by the motion filter as indicators of motion fidelity:

$$K_S = |H_{mf}(j\omega)| \quad \text{with } \omega = 1 \text{ rad/s} \quad (12)$$

$$\phi_S = \angle H_{mf}(j\omega) \quad \text{with } \omega = 1 \text{ rad/s} \quad (13)$$

The motion filter gain and phase distortion at a certain evaluation frequency are, of course, a function of the filter order in addition to the filter parameters. Furthermore, it should be noted that in addition to the filter order, ϕ_S is only affected by the washout dynamics and hence the selected value of ω_n (assuming constant ζ_n and ω_b). The absolute value of $H_{mf}(j\omega)$, however, is not only affected by the filter gain K , but also by the filter break frequency ω_n . This makes K_S a metric that captures, to some extent, the cumulative effect of variations in filter gain and break frequency.

In addition to the motion filter gain and phase distortion at 1 rad/s as given by Eqs. (12) and (13), also other evaluation frequencies – such as 0.5 and 2, and 3 rad/s – were considered as fidelity metrics in this study. This paper, however, will only analyze trends in the dependent measures as a function of K_S and ϕ_S , as the other evaluation frequencies were not found to yield markedly different results for the considered set of experimental measurements.

III.C. Selected Studies

Table 2 presents the details of the ten studies that have so far been included in the data base considered in this paper. Note that in Table 2 a distinction is made between studies that investigated translational and rotational motion cueing. In addition to a short description of the considered control task, Table 2 presents the motion filter dynamics and the different sets of motion filter parameters evaluated in each study. Fig. 2 further depicts the motion filter dynamics evaluated in all studies in the form of the motion filter fidelity criterion proposed by Sinacori,¹⁶ using the definition of the different fidelity regions proposed by Schroeder.²⁰

Note from Table 2 and Fig. 2 that more studies that evaluated pilot tracking behavior with variations in rotational cueing are available. Furthermore, translational motion is typically a lot more problematic with respect to the cueing in flight simulators than rotational motion, due to the large stroke required for presenting, especially low-frequency, aircraft translational motion. This is also observable from Fig. 2, which shows that the motion filter settings that were evaluated for rotational cueing (Fig. 2b) were typically less restrictive – that is, were closer to the dark gray high-fidelity region – than those considered for translational cueing experiments (Fig. 2a).

Table 2. Studies with translational or rotational motion cueing variation included in the literature overview.

Symb.	Ref.	Control Task	Filter	Filter Settings
T.A	11	Conventional aircraft pitch control task (target-following and disturbance-rejection, latter dominant), Cessna Citation controlled element dynamics, varying translational heave cueing, heave cues represent motion wrt. aircraft center of gravity, additional 1-to-1 rotational pitch motion on/off	$K \frac{s^2}{s^2+2\zeta_n\omega_n s+\omega_n^2} \frac{s}{s+\omega_b}$	T.A.1 : $K = 0.0$ T.A.2 : $K = 0.6$ $\omega_n = 1.25$ r/s $\zeta_n = 0.7$ $\omega_b = 0.3$ r/s T.A.3 : $K = 1.0$ $\omega_n = 1.25$ r/s $\zeta_n = 0.7$ $\omega_b = 0.3$ r/s T.A.4 : $K = 0.6$ T.A.5 : $K = 1.0$
T.B	12	Conventional aircraft pitch control task (target-following and disturbance-rejection), Boeing 747 controlled element dynamics, varying translational heave cueing, heave cues represent motion wrt. aircraft center of gravity, additional 1-to-1 rotational pitch motion on/off	$K \frac{s^2}{s^2+2\zeta_n\omega_n s+\omega_n^2} \frac{s}{s+\omega_b}$	T.B.1 : $K = 0.0$ T.B.2 : $K = 0.5$ $\omega_n = 0.5$ r/s $\zeta_n = 0.7$ $\omega_b = 0.3$ r/s T.B.3 : $K = 0.7$ $\omega_n = 1.25$ r/s $\zeta_n = 0.7$ $\omega_b = 0.3$ r/s T.B.4 : $K = 0.3$ $\omega_n = 0.85$ r/s $\zeta_n = 0.7$ $\omega_b = 0.3$ r/s
T.C	15	Helicopter translational heave control task, varying heave motion cueing, separate target-following and disturbance-rejection tasks, helicopter dynamics with "good" and "slightly degraded" vertical responses	$K \frac{s^2}{s^2+2\zeta_n\omega_n s+\omega_n^2}$	T.C.1 : $K = 1.0$ $\omega_n = 0.2$ r/s $\zeta_n = 0.7$ T.C.2 : $K = 1.0$ $\omega_n = 0.5$ r/s $\zeta_n = 0.7$ T.C.3 : $K = 1.0$ $\omega_n = 1.25$ r/s $\zeta_n = 0.7$
T.D	9	Conventional aircraft pitch attitude target-following task, Cessna Citation controlled element dynamics, varying translational heave cueing, heave cues represent motion wrt. aircraft center of gravity, three levels of additional rotational pitch cueing ($K = 0.0, 0.5,$ and 1.0)	$K \frac{s^2}{s^2+2\zeta_n\omega_n s+\omega_n^2}$	T.D.1 : $K = 0.0$ T.D.2 : $K = 0.1$ $\omega_n = 0.75$ r/s $\zeta_n = 0.7$ T.D.3 : $K = 0.5$ $\omega_n = 2.0$ r/s $\zeta_n = 0.7$
R.A	7	Conventional aircraft roll control task (combined target-following and disturbance-rejection task), Cessna Citation controlled element dynamics, varying rotational roll cueing, no compensation for lateral specific force cues resulting from simulator roll	$K \frac{s}{s+\omega_n}$	R.A.1 : $K = 0.0$ R.A.2 : $K = 0.5$ $\omega_n = 0.5$ r/s R.A.3 : $K = 1.0$ $\omega_n = 0.5$ r/s R.A.4 : $K = 1.0$ $\omega_n = 0.0$ r/s
R.B	10	Pitch attitude control task (dominant target-following and dominant disturbance-rejection tasks performed separately), double integrator controlled element dynamics, pure scaling of the supplied pitch motion cues (no washout)	K	R.B.1 : $K = 0.25$ R.B.2 : $K = 0.5$ R.B.3 : $K = 0.75$ R.B.4 : $K = 1.0$
R.C	8	Roll attitude control task (combined target-following and disturbance-rejection task), two controlled elements: $K/(s(s+10))$ and K/s^2 , priority III conditions	$K \frac{s}{s+\omega_n}$	R.C.1 : $K = 1.0$ $\omega_n = 0.5$ r/s R.C.2 : $K = 1.0$ $\omega_n = 1.0$ r/s R.C.3 : $K = 1.0$ $\omega_n = 2.0$ r/s
R.D	13	Two-axis pitch and yaw attitude disturbance-rejection task, single integrator controlled element dynamics in both axes, pure scaling of the supplied pitch motion cues (no washout)	K	R.D.1 : $K = 0.0$ R.D.2 : $K = 0.0625$ R.D.3 : $K = 0.125$ R.D.4 : $K = 0.25$ R.D.3 : $K = 0.5$ R.D.4 : $K = 1.0$
R.E	4	Conventional aircraft roll attitude control task (combined target-following and disturbance-rejection task), controlled element representative of a fighter aircraft	$K \frac{s}{s+\omega_n}$ and $K \frac{s^2}{s^2+2\zeta_n\omega_n s+\omega_n^2}$	R.E.1 : $K = 1.0$ R.E.2 : $K = 1.2$ $\omega_n = 0.85$ r/s $\zeta_n = 0.7$ 2 nd order R.E.3 : $K = 1.0$ $\omega_n = 1.0$ r/s R.E.4 : $K = 0.7$ $\omega_n = 0.4$ r/s R.E.5 : $K = 0.53$ R.E.6 : $K = 0.0$
R.F	14	Conventional aircraft pitch and roll attitude disturbance-rejection tasks (performed separately), controlled element representative of a DC9-10 in the landing/approach configuration	$K \frac{s^2}{s^2+2\zeta_n\omega_n s+\omega_n^2}$	R.F.1 : $K = 1.0$ $\omega_n = 0.2$ r/s $\zeta_n = 1.0$ R.F.2 : $K = 1.0$ $\omega_n = 0.25$ r/s $\zeta_n = 1.0$ R.F.3 : $K = 1.0$ $\omega_n = 0.5$ r/s $\zeta_n = 1.0$ R.F.4 : $K = 0.0$

III.D. Pilot Model Tuning Rule Development

III.D.1. Data Normalization

The goal of this study is to obtain a quantitative indication of the magnitude of pilot behavioral adjustments in response to the presence of a motion filter with certain dynamics. The collected behavioral measurements from the studies listed in Table 2 will therefore be used to see if consistent variations in any of the dependent measures listed in Table 1 and any of the predictor variables introduced in Section III.B can be found. For a dependent measure Z and a predictor variable Y , this means we are looking for a prediction equation $Z(Y)$.

It should be noted that differences in the defining characteristics of the compensatory control tasks (for example, controlled element dynamics, forcing function signals, and adopted display formats) naturally lead to large offsets in some of the dependent measures listed in Table 1. For instance, a controlled element with double integrator dynamics as used in Ref. 10 requires markedly more pilot lead equalization (higher T_L) than typical aircraft pitch and roll dynamics as controlled in the experiment of Ref. 14. As the relative change in the considered dependent measures due to changes in motion filter dynamics is of interest to this study, the data from all dependent measures has been normalized with the mean of this dependent measure over all conditions for each experiment. For values of a dependent measure Z taken from an experiment with N_z different motion filter conditions, this gives:

$$\bar{Z}[n] = \frac{Z[n]}{\frac{1}{N_z} \sum_{k=1}^{N_z} Z[k]} \quad \text{with } n = 1 \dots N_z \quad (14)$$

To illustrate the necessity of this normalization, Fig. 3 shows a side-by-side comparison of the raw data and the result of the normalization of all measurements for the pilot visual lead time constant T_L . Note from Fig. 3b that due to the normalization according to Eq. (14), the normalized dependent measure represents the percentage-wise variation in the dependent measure over the range of the selected predictor.

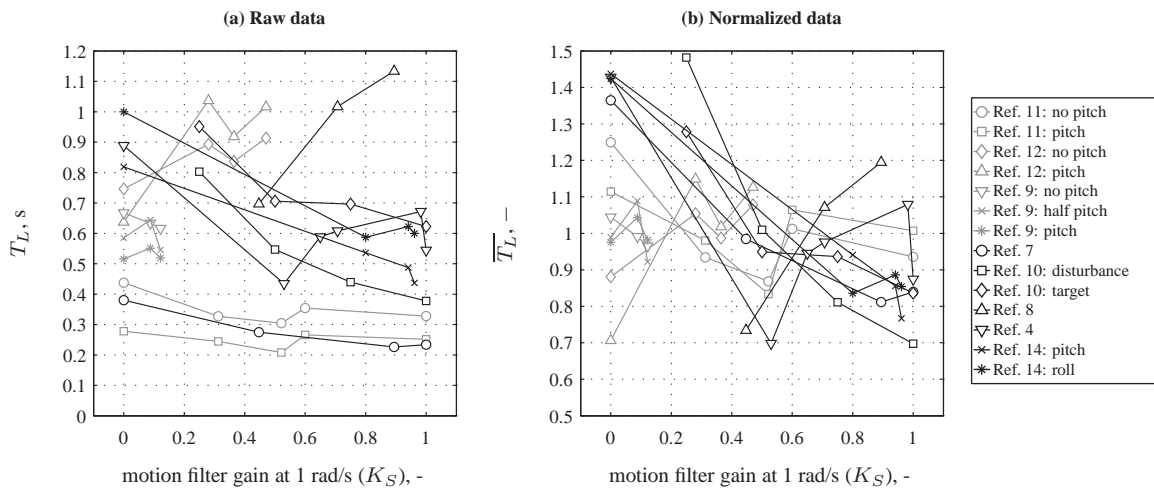


Figure 3. Example of data normalization for pilot visual lead time constant T_L according to Eq. (14).

III.D.2. Linear Regression Modeling

For all dependent measures, the normalized data were tested for correlation with the considered measures of motion filter characteristics (see Section III.B) by calculating Pearson's correlation coefficient R .²⁷ For absolute values of R of 0.3 and higher, the correlation between both variables was defined to be strong enough ("medium" correlation or stronger²⁷) to allow for modeling of the trend in the data using a linear regression. This linear regression represents a relation between the normalized dependent measure \bar{Z} and the independent (predictor) variable Y given by:

$$\bar{Z}(Y) = \beta(Y - Y_{ref}) + \alpha_{Y_{ref}} \quad (15)$$

In Eq. (15), Y_{ref} represents the reference value of the predictor variable Y , with respect to which the trend in Z is to be predicted. The symbols β and $\alpha_{Y_{ref}}$ are the linear regression coefficient and offset, which are determined by

fitting the model of Eq. (15) to the normalized data using a least-squares fitting procedure. It should be noted that for data as presented in Fig. 3b a different choice in Y_{ref} (for instance $K_S = 0$ or $K_S = 1$) affects the value of $\alpha_{Y_{ref}}$ for the corresponding regression model, but not the value of β . When converting Eq. (15) back to the non-normalized dependent measure $Z(Y)$ (note that $\alpha_{Y_{ref}} = \bar{Z}(Y_{ref})$ and use Eq. (14)) an equation results that can be used for linear prediction of the considered dependent measure based on the parameters of the fitted linear regression:

$$Z(Y) = Z(Y_{ref}) \left[\frac{\beta}{\alpha_{Y_{ref}}} (Y - Y_{ref}) + 1 \right] \quad (16)$$

In Eq. (16), $Z(Y_{ref})$ represents the value of the dependent measure at the reference value of Y . For a control task where pilot behavior and pilot-vehicle system performance and crossover characteristics are known for a reference predictor setting, $Z(Y_{ref})$, this allows for prediction of changes in Z for other values of Y according to Eq. (16). Note from Eq. (16) that the coefficient that defines the magnitude of the change in Z due to a variation in Y is given as the fraction of β and $\alpha_{Y_{ref}}$, and hence is dependent on the choice of the reference predictor value Y_{ref} .

IV. Results

IV.A. Predictor Variable Selection

As explained in Section III.D, four different variables were considered as predictors for observed trends in the dependent measures listed in Table 1: the motion filter gain K , the (dominant) motion filter break frequency ω_n , the motion filter gain at 1 rad/s K_S , and the motion filter phase distortion at 1 rad/s ϕ_S . For all combinations of dependent measure and predictor variables plots as those depicted in Fig. 3 were evaluated to investigate possible correlation between the two considered metrics. Furthermore, the correlation coefficients R calculated for all considered combinations of dependent measures and predictors were calculated and are presented in Table 3.

Table 3. Correlation coefficients for all considered combinations of dependent measure and predictor. Bold font indicates $|R| > 0.3$.

Predictor	Dependent Measures															Mean $ R $
	σ_e^2	σ_u^2	$\omega_{c,d}$	$\omega_{c,t}$	$\varphi_{m,d}$	$\varphi_{m,t}$	K_v	T_L	T_I	K_m	τ_v	τ_m	ω_{nm}	ζ_{nm}	$K_v T_L$	
K	-0.30	0.53	0.37	-0.09	-0.02	0.05	0.40	-0.33	-0.62	-0.11	0.32	-0.42	0.28	0.25	0.01	0.27
ω_n	0.47	0.12	-0.61	0.57	0.49	-0.47	-0.15	-0.07	-0.23	0.32	-0.41	-0.22	0.06	-0.50	-0.40	0.34
K_S	-0.60	0.54	0.69	-0.26	-0.30	0.28	0.60	-0.49	-0.33	-0.11	0.40	-0.30	0.35	0.27	0.09	0.37
ϕ_S	0.18	-0.17	-0.52	0.38	0.41	-0.42	-0.16	0.05	-0.57	-0.09	-0.25	-0.05	-0.22	-0.03	-0.09	0.24

Each column in Table 3 presents the values of R for one of the considered dependent measures (see Table 1). The final column of Table 3 shows the average absolute correlation coefficient calculated across all dependent measures. As can be verified from this final column, the strongest average $|R|$ across all dependent measures is present for the motion filter gain at 1 rad/s (K_S). Based on this strongest average correlation across all dependent measures – although a number of medium and strong correlations are also found for the other predictors and considering that the average correlation coefficient for ω_n is nearly as high as found for K_S – the choice is made in this paper to focus on K_S as the most promising predictor variable.

Another reason for favoring K_S as the predictor in this paper can be observed from Table 2 and Fig. 2. Some of the included studies considered pure-gain motion filter dynamics K ,^{10,13} so no variation in ω_n and ϕ_S was available for these experiments. Furthermore, as explained in Section III.B, K_S is the only considered predictor variable that is a function of both the motion filter gain (K) and filter characteristics (ω_n). Though different combinations of K and ω_n can still give the same value for this predictor, K_S is still selected here as the most promising of the considered predictor variables because of this property. All results presented in this section, and also the derived pilot model tuning rules, will utilize K_S as the predictor.

It should be noted that the frequency of 1 rad/s at which K_S was selected for correspondence with the fidelity criteria of Sinacori¹⁶ and Schroeder,²⁰ but that evaluation of the filter dynamics at other frequencies in the range of interest to manual control (see Section III.B) yielded highly similar results.

For prediction of changes in behavior due to variations in motion cueing, here the condition where no motion filter is present, yielding 1-to-1 presentation of motion cues, will be considered as the baseline. For the selected predictor variable this corresponds to the case where $K_S = 1$. Naturally, tuning rules could also be defined with respect to the no-motion case ($K_S = 0$), but for interpreting the effects of motion filters on pilot behavior, the chosen convention

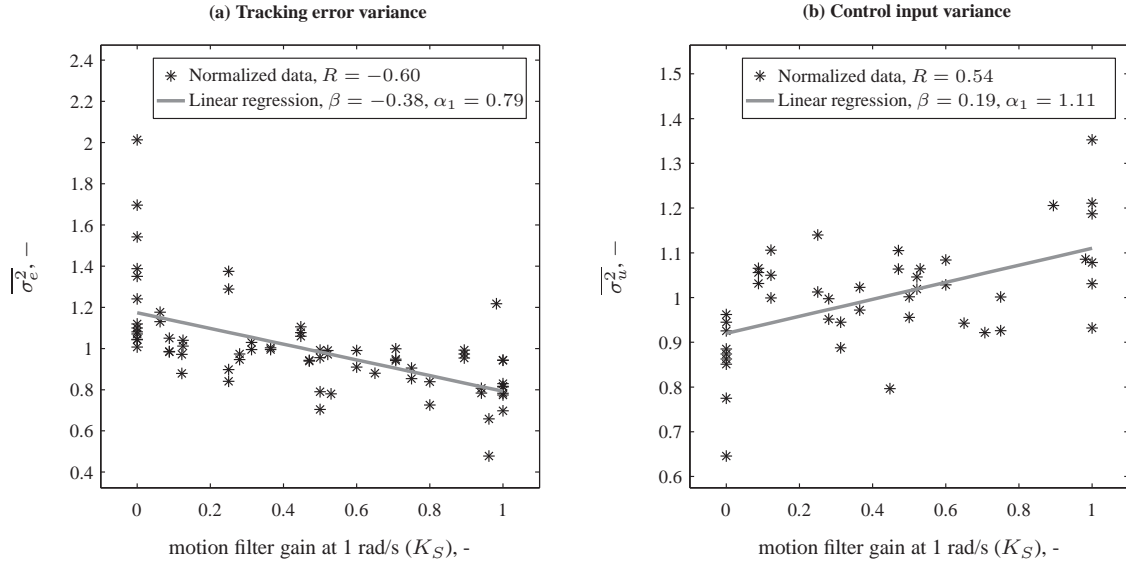


Figure 4. Variation in tracking performance and control activity as a function of K_S .

was thought to be more intuitive. Substitution of $Y = K_S$ and $Y_{ref} = K_{S_{ref}} = 1$ in Eq. (16) results in the following structure for the linear prediction equations that will be derived in this paper:

$$Z(K_S) = Z(1) \left[\frac{\beta}{\alpha_1} (K_S - 1) + 1 \right] \quad (17)$$

In Eq. (17), $Z(1)$ represents the value of the considered dependent measure for the reference case where $K_S = 1$. The symbols β and α_1 are the parameters of the fitted linear regression model (see Section III.D.2).

IV.B. Notable Trends in Dependent Measures

IV.B.1. Tracking Performance and Control Activity

Fig. 4 presents the normalized tracking error and control input variance data for the studies included in this overview. Fig. 4 depicts the normalized data for both dependent measures as black markers, while the linear regression that was fit through the data is shown as a solid gray line.

As can be verified from Fig. 4, for both σ_e^2 and σ_u^2 a strong correlation ($|R| > 0.5$) with the variation in K_S is present. Fig. 4 shows that an increase in K_S is found to yield improved tracking performance (lower σ_e^2) and increased control activity (higher σ_u^2). Substitution of the fitted values of β and α_1 (indicated in the bottom legend entries in Fig. 5) in the prediction equation given by Eq. (17) yields the following tuning rules for σ_e^2 and σ_u^2 :

$$\sigma_e^2(K_S) = \sigma_e^2(1) [-0.48 (K_S - 1) + 1] \quad (18)$$

$$\sigma_u^2(K_S) = \sigma_u^2(1) [0.17 (K_S - 1) + 1] \quad (19)$$

In Eqs. (18) and (19), $\sigma_e^2(1)$ and $\sigma_u^2(1)$ represent the level of tracking performance and control activity for the case where $K_S = 1$, respectively. As can be verified from Fig. 4a and Eq. (18), tracking performance on average worsens by 48% for $K_S = 0$ compared to $K_S = 1$. Similarly, Eq. (19) shows that control input variance is found to decrease by 17% under the same variation of K_S .

IV.B.2. Pilot-Vehicle System Crossover Frequencies

For the phase margins of the disturbance and target open-loop responses (Eqs. (1) and (2)) – $\varphi_{m,d}$ and $\varphi_{m,t}$, respectively – no $|R| > 0.3$ with K_S was observed, as can be verified from Table 3. For the corresponding crossover frequencies $\omega_{c,d}$ and $\omega_{c,t}$ the normalized collected data and fitted linear regressions are depicted in Fig. 5. Fig. 5a

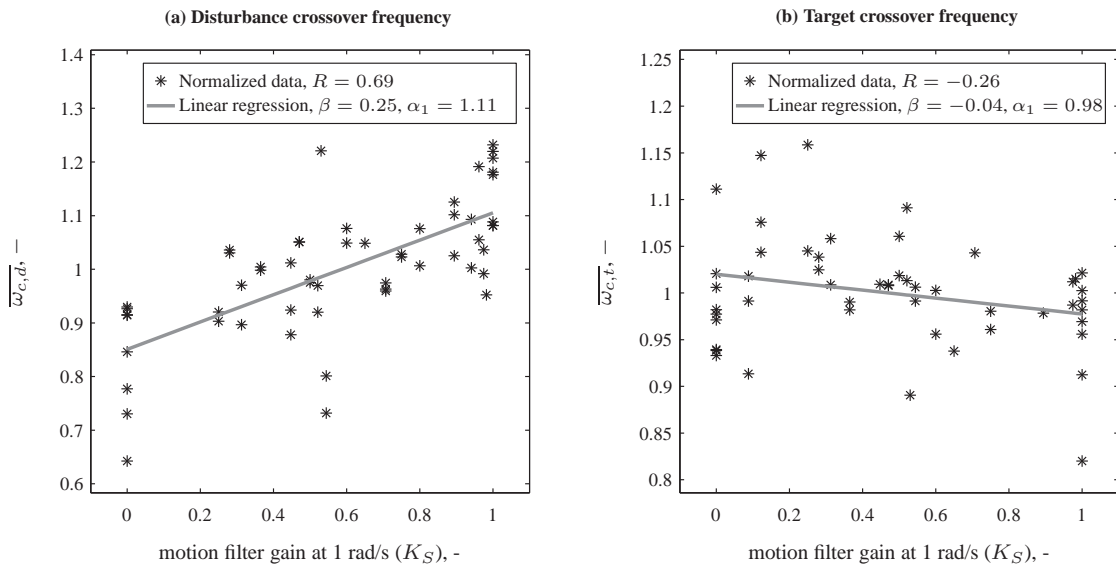


Figure 5. Disturbance and target loop crossover frequency as a function of K_S .

shows a strong positive correlation between $\omega_{c,d}$ and K_S , indicating disturbance crossover frequencies are typically found to increase with increasing K_S . Though not a medium correlation, as $|R| < 0.3$, the target crossover frequency data presented in Fig. 5b still show a much smaller opposite trend with K_S . As these trends are consistent with the results reported in a number of the individual studies that were included,^{10,11,15,25} the following tuning rules are defined for $\omega_{c,d}$ and $\omega_{c,t}$:

$$\omega_{c,d}(K_S) = \omega_{c,d}(1) [0.23(K_S - 1) + 1] \quad (20)$$

$$\omega_{c,t}(K_S) = \omega_{c,t}(1) [-0.043(K_S - 1) + 1] \quad (21)$$

Eq. (20) indicates a variation of around 23% over the range of K_S values from 0 to 1 for $\omega_{c,d}$. For the target crossover frequency $\omega_{c,t}$, see Eq. (21), this variation is found to remain below 5%.

IV.B.3. Pilot Behavioral Parameters

Fig. 6 shows the normalized measurement data as a function of K_S for the five most interesting pilot model parameters with respect to the effects of motion cueing variations: the pilot visual gain K_v , the pilot visual lead time constant T_L , the pilot motion gain K_m , and the pilot visual and motion time delays, τ_v and τ_m , respectively. For the remaining parameters, either too little data was thought to be available for identifying consistent trends (T_I , only Refs. 11 and 12 provide data) or no consistent or meaningful effects as a function of K_S were found ($K_v T_L$, ω_{nm} , and ζ_{nm} , see Table 3).

Fig. 6 shows a strong positive correlation with K_S for the pilot visual gain K_v , while for T_L and τ_v medium values for the correlation coefficient are found ($0.3 > R \geq 0.5$). Pilot visual gains are consistently found to be higher for higher values of K_S , indicating pilots respond with a higher gain to visually presented tracking errors when motion cueing is of higher fidelity, a finding that is indeed reported in many studies. Here, an average change in K_v of nearly 20% is found over the full range of K_S .

One of the most consistent effects that is reported in many studies that investigate the effects of motion feedback on manual control behavior is that the presence of motion feedback allows for a reduction in the amount of visual lead equalization that pilots need to adopt.^{7,10,11,24-26,28} This reduction in visual lead stems from the fact that the motion cues, which are, for instance, perceived with the vestibular system, provide information on the rates of the controlled element state directly, thereby removing the requirement to generate lead visually.^{3,24} Fig. 6b shows that this is also apparent from the collected data of all experiments listed in Table 2. Values for the visual lead time constant T_L are seen to increase with decreasing K_S , with a total variation of 29% over the full range of $K_S = 0$ to 1.

The final correlation with $R > 0.3$ is found for the pilot visual delay τ_v . Even though the trend in this dependent measure is not as large as those found for K_v and T_L (only 7% variation for K_S ranging from 0 to 1), still a highly

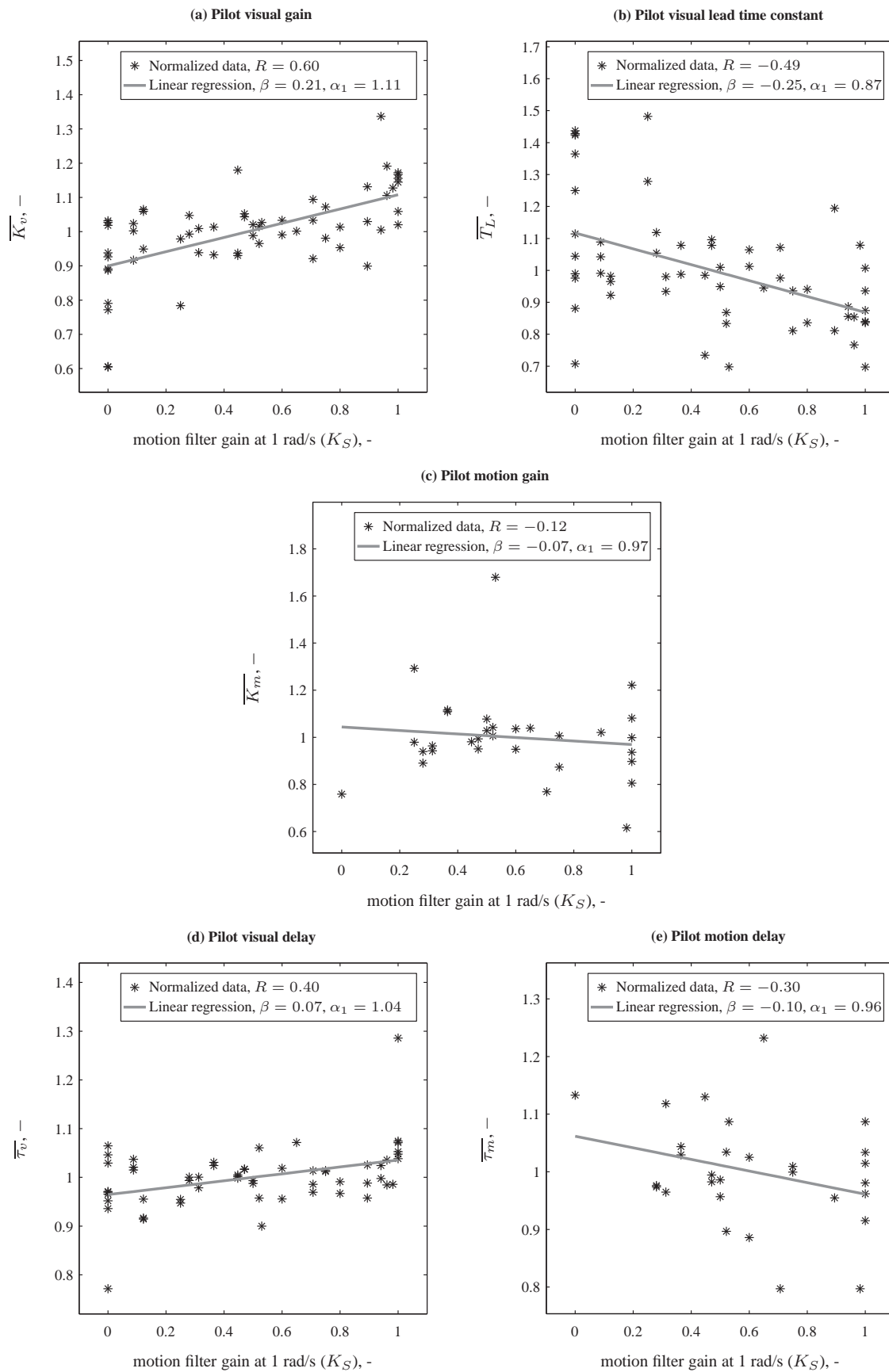


Figure 6. Variation in important multimodal pilot model parameters as a function of K_S .

consistent increase in τ_v is observed with increasing K_S . This effect is often seen to occur in series with a reduction in the amount of visual lead equalization (lower T_L), and is believed to result from the fact that due to the added information from motion feedback, a control strategy that requires less workload, but induces more high-frequency phase lag in the pilot visual control response $H_{p_v}(j\omega)$, is permissible without significant effect on the dominant closed-loop characteristics.

The collected data for the pilot motion gain K_m and τ_m are not found to yield values of $|R| > 0.3$ (though τ_m is close). Especially the nearly constant values of K_m under a variation of K_S are notable, as this implies that pilots appear to be unable to increase their K_m to compensate for reductions in motion cue magnitude, as suggested in Section II.C. These results for the pilot motion gain therefore suggest a reducing contribution of motion feedback to pilot control behavior with reducing K_S .

The linear pilot model parameter tuning equations that can be derived from the linear regression models fit to the data presented in Fig. 6 are given by:

$$K_v(K_S) = K_v(1) [0.19 (K_S - 1) + 1] \quad (22)$$

$$T_L(K_S) = T_L(1) [-0.29 (K_S - 1) + 1] \quad (23)$$

$$K_m(K_S) = K_m(1) \quad (24)$$

$$\tau_v(K_S) = \tau_v(1) [0.069 (K_S - 1) + 1] \quad (25)$$

$$\tau_m(K_S) = \tau_m(1) \quad (26)$$

Again, Eqs. (22) to (26) indicate the change in the values of K_v to τ_m relative to the case where $K_S = 1$. Hence, the parameters $K_v(1)$ to $\tau_m(1)$ indicate the values of these pilot model parameters that would be suitable for pilot control behavior when $K_S = 1$.

V. Discussion

This paper presented the first results of an effort to develop some rudimentary tuning rules for adaptation of pilot behavioral tracking model parameters to variations in motion feedback. Data from a number of studies that investigated the effects of variations in motion cueing settings on pilot tracking behavior and performance were compiled, compared to selected measures of motion cueing fidelity, and used to fit linear regression models for those combinations of predictor variables and dependent measures for which a sufficiently strong correlation was observed. Using the motion filter gain at 1 rad/s as the predictor variable, a set of mathematical equations was obtained that allows for tuning multimodal pilot model parameters to a selected motion filter setting, granted that the pilot dynamics for the control task where no motion filter is present in the motion feedback path are known.

The choice of the predictor variable to use for pilot model tuning rules as attempted in this paper is a very important and complicated one, as it essentially requires a single numerical metric that summarizes the total motion filter dynamics. Here the motion filter gain at 1 rad/s (K_S) was selected as the most promising predictor variable, as this metric is indeed affected by both variations in motion cue scaling (motion filter gain K) and motion cue filtering (motion filter break frequency ω_n). However, it should be noted that this choice of metric also has some drawbacks. For instance, the choice of the 1 rad/s evaluation frequency implies that all motion filters for which $\omega_n \ll 1$ rad/s essentially become pure gain attenuation filters, as in that case K_S is not affected by the filter dynamics governed by ω_n . Therefore, a more in-depth investigation of this effect of the frequency at which K_S is evaluated than described here, and the testing of further possible predictor variables, is thought to be valuable to the work described in this paper.

In this paper, only linear regression models were fit to the collected data, thereby yielding a set of linear prediction or interpolation equations to adjust pilot model parameters. In reality, it is unlikely that only linear variations of parameters that define pilot control behavior with respect to a selected predictor variable will occur. However, for investigating for which dependent measures this might be appropriate and for deriving valid higher-order prediction models from collected data as used in this study, a significantly larger number of available measurements is needed.

The observed trends in the dependent measures for which tuning equations have been derived in this paper are mostly highly consistent over the different experiments considered in this study. There are, however, some exceptions that result from differences in the defining elements of the considered control tasks, which should be taken into account

when applying the equations from this paper. One notable example is the observed reduction in the pilot visual lead time constant T_L with increasing K_S . This trend is consistent over studies in which the controlled element state is the dominant motion cue that is perceivable to the pilot. For control tasks for which this is not the case, most notably for pitch tracking tasks with conventional aircraft as considered in a number of previous studies,^{9,12,25} where heave motion is the dominant motion cue rather than rotational pitch motion, an opposite trend in T_L is observed. This is believed to be a result of the fact that this heave motion provides less useful motion feedback to pilots than only rotational pitch motion would. Such effects, however, are not yet explicitly included in the tuning rules as described in this paper.

It should be noted that predicting human manual control behavior is always going to remain a difficult problem, mainly due to the sheer number of factors that affect the adopted control strategy.² Hence, the equations for predicting changes in tracking performance, pilot-vehicle crossover frequencies, and behavioral pilot model parameters as developed in this paper should always be used with some caution. The tuning rules developed in this paper will be updated when new sets of data are added to the database. In addition, future work will include applying the rules formulated in this paper to an experiment that is planned for the end of 2011, for which we will attempt to measure pilot tracking behavior for a large variation in motion filter parameter settings and motion filter orders.

VI. Conclusions

Using data from ten different investigations into the effects of motion filter characteristics on pilot tracking behavior and performance, this paper developed a rudimentary set of tuning rules that can be used to adjust pilot model parameters to a selected motion filter setting. The motion filter gain at 1 rad/s, which is also used as a metric in a well-known criterion for evaluating simulator motion cueing fidelity, was found to be the most promising metric to use for the prediction of changes in pilot control strategy. Consistent changes in pilot behavior due to variations in motion filter dynamics that were revealed for the data used in this study include increased pilot visual gains, reduced pilot visual lead equalization, and increased pilot visual response delays when the predicted level of motion fidelity is increased. Linear regression models were fit to data for these parameters to define a set of mathematical equations that can be used to predict the values of these parameters for a specific motion filter setting.

Acknowledgments

This research was supported by the Dutch Technology Foundation (STW), the applied science division of The Netherlands Organization for Scientific Research (NWO), and the technology program of the Ministry of Economic Affairs.

References

- ¹McRuer, D. T., Graham, D., Krendel, E. S., and Reisener, W. J., "Human Pilot Dynamics in Compensatory Systems, Theory Models and Experiments with Controlled Element and Forcing Function Variations," Tech. Rep. AFFDL-TR-65-15, Air Force Flight Dynamics Laboratory, 1965.
- ²McRuer, D. T. and Jex, H. R., "A Review of Quasi-Linear Pilot Models," *IEEE Transactions on Human Factors in Electronics*, Vol. HFE-8, No. 3, Sept. 1967, pp. 231–249.
- ³Shirley, R. S. and Young, L. R., "Motion Cues in Man-Vehicle Control – Effects of Roll-Motion Cues on Human Operator's Behavior in Compensatory Systems with Disturbance Inputs," *IEEE Transactions on Man-Machine Systems*, Vol. 9, No. 4, Dec. 1968, pp. 121–128.
- ⁴Jex, H. R., Magdaleno, R. E., and Junker, A. M., "Roll Tracking Effects of G-vector Tilt and Various Types of Motion Washout," *Proceedings of the Fourteenth Annual Conference on Manual Control*, 1978, pp. 463–502.
- ⁵Schroeder, J. A. and Grant, P. R., "Pilot Behavioral Observations in Motion Flight Simulation," *Proceedings of the AIAA Guidance, Navigation, and Control Conference, Toronto, Canada, Aug. 2-5*, No. AIAA-2010-8353, 2010.
- ⁶Grant, P. R. and Schroeder, J. A., "Modelling Pilot Control Behaviour for Flight Simulator Design and Assessment," *Proceedings of the AIAA Guidance, Navigation, and Control Conference, Toronto, Canada, Aug. 2-5*, No. AIAA-2010-8356, 2010.
- ⁷Pool, D. M., Zaai, P. M. T., Damveld, H. J., Van Paassen, M. M., and Mulder, M., "A Cybernetic Approach to Assess Flight Simulator Motion Fidelity," *Proceedings of the 11th IFAC/IFIP/IFORS/IEA Symposium on Analysis, Design, and Evaluation of Human-Machine Systems, August 31–September 3, 2010, Valenciennes, France*, 2010.
- ⁸Stapleford, R. L., Peters, R. A., and Alex, F. R., "Experiments and a Model for Pilot Dynamics with Visual and Motion Inputs," Tech. Rep. NASA CR-1325, Systems Technology, Inc., Hawthorne (CA), 1969.
- ⁹Steurs, M., Mulder, M., and Van Paassen, M. M., "A Cybernetic Approach to Assess Flight Simulator Fidelity," *Proceedings of the AIAA Modelling and Simulation Technologies Conference and Exhibit, Providence (RI)*, No. AIAA-2004-5442, 2004.
- ¹⁰De Vroome, A. M., Valente Pais, A. R., Pool, D. M., Van Paassen, M. M., and Mulder, M., "Identification of Motion Perception Thresholds in Active Control Tasks," *Proceedings of the AIAA Modeling and Simulation Technologies Conference and Exhibit, Chicago (IL)*, No. AIAA-2009-

6243, Aug. 2009.

¹¹Pool, D. M., Zaal, P. M. T., Van Paassen, M. M., and Mulder, M., "Effects of Heave Washout Settings in Aircraft Pitch Disturbance Rejection," *Journal of Guidance, Control, and Dynamics*, Vol. 33, No. 1, 2010, pp. 29–41.

¹²Van Wieringen, A. T., Pool, D. M., Van Paassen, M. M., and Mulder, M., "Effects of Heave Washout Filtering on Motion Fidelity and Pilot Control Behavior for a Large Commercial Airliner," *AIAA Modeling and Simulation Technologies Conference and Exhibit, Portland (OR), August 8–11, 2011* (submitted for publication).

¹³Bergeron, H. P., "Investigation of Motion Requirements in Compensatory Control Tasks," *IEEE Transactions on Man-Machine Systems*, Vol. MMS-11, No. 2, June 1970, pp. 123–125.

¹⁴Van Gool, M. F. C., "Influence of Motion Washout Filters on Pilot Tracking Performance," *Piloted Aircraft Environment Simulation Techniques*, No. AGARD-CP-249, 1978, pp. 19–1 – 19–5.

¹⁵Bray, R. S., "Visual and Motion Cueing in Helicopter Simulation," Technical Memorandum NASA-TM-86818, NASA Ames Research Center, Moffett Field (CA), Sept. 1985.

¹⁶Sinacori, J. B., "The Determination of Some Requirements for a Helicopter Research Simulation Facility," Tech. Rep. NASA-CR-152066, Systems Technology Inc., Sept. 1977.

¹⁷Schmidt, S. F. and Conrad, B., "Motion Drive Signals for Piloted Flight Simulators," Tech. Rep. NASA CR-1601, National Aeronautics and Space Administration, Ames Research Center, 1970.

¹⁸Reid, L. D. and Nahon, M. A., "Flight Simulation Motion-Base Drive Algorithms. Part 1: Developing and Testing the Equations," Tech. Rep. UTIAS 296, University of Toronto, Institute for Aerospace Studies, Dec. 1985.

¹⁹Telban, R. J., Wu, W., and Cardullo, F. M., "Motion Cueing Algorithm Development: Initial Investigation and Redesign of the Algorithms," Contractor Report NASA-CR-2000-209863, NASA Langley Research Center, Hampton (VA), March 2000.

²⁰Schroeder, J. A., "Helicopter Flight Simulation Motion Platform Requirements," Tech. Rep. NASA-TP-1999-208766, National Aeronautics and Space Administration, July 1999.

²¹Hess, R. A., Malsbury, T., and Atencio, Jr., A., "Flight Simulator Fidelity Assessment in a Rotorcraft Lateral Translation Maneuver," *Journal of Guidance, Control, and Dynamics*, Vol. 16, No. 1, 1993, pp. 79–85.

²²Hess, R. A. and Marchesi, F., "Analytical Assessment of Flight Simulator Fidelity Using Pilot Models," *Journal of Guidance, Control, and Dynamics*, Vol. 32, No. 3, May/June 2009, pp. 760–770.

²³Advani, S. K. and Hosman, R. J. A. W., "Towards Standardizing High-Fidelity Cost-Effective Motion Cueing in Flight Simulation," *Proceedings of the Royal Aeronautical Society Flight Simulation Conference, London (UK), November 7-8, 2006*.

²⁴Hosman, R. J. A. W., *Pilot's Perception and Control of Aircraft Motions*, Ph.D. thesis, Delft University of Technology, Faculty of Aerospace Engineering, 1996.

²⁵Zaal, P. M. T., Pool, D. M., De Bruin, J., Mulder, M., and Van Paassen, M. M., "Use of Pitch and Heave Motion Cues in a Pitch Control Task," *Journal of Guidance, Control, and Dynamics*, Vol. 32, No. 2, 2009, pp. 366–377.

²⁶Pool, D. M., Zaal, P. M. T., Damveld, H. J., Van Paassen, M. M., Van der Vaart, J. C., and Mulder, M., "Modeling Wide Frequency Range Pilot Equalization for Control of Aircraft Pitch Dynamics," *Journal of Guidance, Control, and Dynamics*, (to be published).

²⁷Field, A., *Discovering Statistics Using SPSS*, ISM Introducing Statistical Methods, SAGE Publications Ltd., 2nd ed., 2005.

²⁸Van der Vaart, J. C., *Modelling of Perception and Action in Compensatory Manual Control Tasks*, Ph.D. thesis, Delft University of Technology, Faculty of Aerospace Engineering, 1992.